Evidence for multipolar charge distribution in falling water drops

José A. Fornés[a)]
Instituto de Matemática e Física, Universidade Federal de Goiás, Caixa Postal 131, 74001-970, Goiânia, GO, Brazil

Joaquim Procopio
Instituto de Ciências Biomédicas, Universidade de São Paulo, Caixa Postal 66208, 05508-970, São Paulo, SP, Brazil

José C. Sartorelli
Instituto de Física, Universidade de São Paulo, Caixa Postal 66318, 05389-970, São Paulo, SP, Brazil

(Received 18 June 1996; accepted for publication 8 August 1996)

A method for producing water drops with very small net charge (few fC) was employed in conjunction with a sensing device, in order to identify the electric signals produced by falling water drops. The sensing device consists of a wire loop hooked to a patch-clamp amplifier set into voltage-clamp mode. Water drops with very small net charge produce a negligible signal at the sensing device but when falling through a horizontal charged capacitor they produce well-defined and reproducible signals which are proportional to the capacitor voltage. The experimental curves can be fitted to the theoretical ones considering the drop as possessing a multipolar charge distribution. There is evidence that this distribution is due to the contribution of the field-oriented water molecules multipoles. © *1996 American Institute of Physics.* [S0021-8979(96)01422-3]

I. INTRODUCTION

Water drops and droplets are known to possess an electrical charge. This is due mostly to electrification during formation or during flight as in the case of rain drops. Evidences that water drops possess charge are rather old (Kelvin 1860).[1] Electrical charge determination in single water drops has been undertaken since the 1920s in rain drops and innumerable other measurements have been made since then, using different instruments. Despite extensive investigation on the subject of drop electrification very scarce information is available concerning the charge distribution within falling or immobile water drops. This is justifiable in view of the difficulties in constraining a water drop without charge exchange. However, even after the advent of the space shuttle scientific missions at microgravity conditions no additional information has come up concerning charge distribution in water drops suspended or falling in air. We have been able to control (see methods) the charge with which drops are produced with a reasonable degree of accuracy. In this way we could produce drops of nearly zero net charge. When such zero charge drops fall through a time constant and vertically directed electric field, a detector, placed inside the field lines, reveals a pattern which is compatible with a multipolar charge distribution.

II. EXPERIMENTAL SETUP AND METHODS

The experimental setup consists of four independent sets of devices: Device 0 is the dropper reservoir; device 1 establishes a voltage in the region of drop formation and imposes a given electrical charge in the drop; device 2 is a charged capacitor across the path of the falling drop; and device 3 measures the electrical effects produced by the passing drop (see Fig. 1).

Device 0 is a glass reservoir containing about 300 ml of water and opened in the bottom to a no. 8 stainless-steel disposable needle, cut flat. The drops are formed at the needle tip due to the passive pressure of the water in the reservoir, at a rate of about 1 drop/s. The needle is grounded to the cage carcass.

Device 1 consists of a aluminum ring enclosing the drop at its formation and creating a cylindrical cavity of 10 mm diameter and 12 mm height which encloses the drop. This forces the still pedunculated drop to acquire a given charge in order to keep its potential at the reservoir potential which is zero. In this way the potential produced by the charge distribution in the drop and the potential produced by the charge distribution in the ring summate to zero. By changing the voltage of the surrounding ring we were able to precisely control the charge of the free drop. When the drop frees from the needle it keeps the original charge throughout its short flight.

Device 2 consists of a parallel-plate (circular) capacitor with a 67 mm separation between the plates and diameter of 140 mm. The drop enters and exits the capacitor through 8-mm-wide holes in the center of the plates. A potential difference can be applied across the plates by connecting the lower plate to a dc source and the upper plate to ground.

Device 3 is the measuring probe (henceforth called simply ''sensor'') and consists of a copper wire loop of circular aspect of 2.8 mm radius, and cross section of about 0.2 mm, across which the drops fall. The ring is connected to the 10 GΩ probe of a model 8900 Dagan patch-clamp amplifier, in the current-to-voltage configuration and set to voltage-clamp mode at voltage zero. There is never direct physical contact between the probe and the drop, the coupling being only capacitive.

In the voltage-clamp mode the apparatus maintains the sensor continually at zero potential, by injecting current I_{inj} through its feedback resistance R_{FB} (in this case equal to

a)Author to whom correspondence should be addressed.

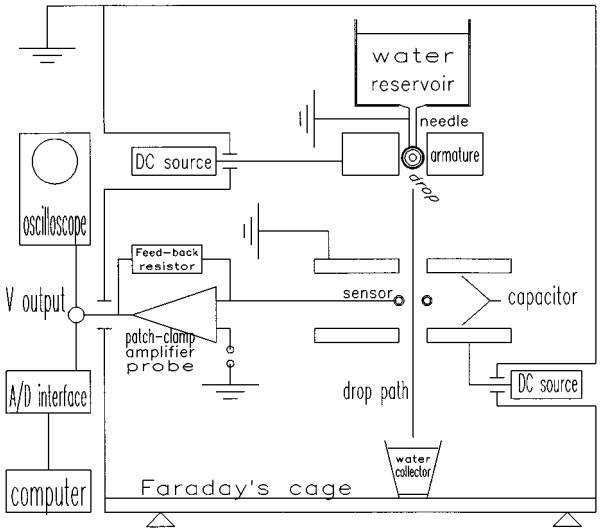

FIG. 1. Experimental setup.

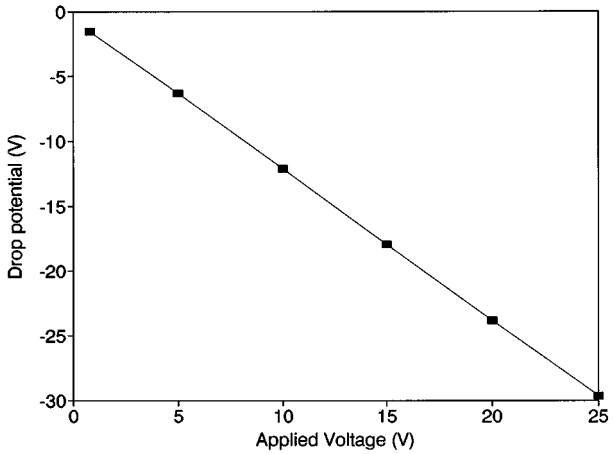

FIG. 2. Correlation between ring potential and drop potential as inferred from drop charge and diameter.

$5\times10^{10}\ \Omega$) which constitutes the amplifier gain. The product $I_{\text{inj}}\times R_{\text{FB}}$ gives the voltage output of the patchclamp amplifier measured in volts V_{output}. The following relations then hold:

$$I_{\text{inj}}=C\left(\frac{d\Phi}{dt}\right)_{\text{expt}}, \tag{1}$$

$$V_{\text{out}}=R_{\text{FB}}I_{\text{inj}}, \tag{2}$$

From Eqs. 1 and 2 we obtain

$$\left(\frac{d\Phi}{dt}\right)_{\text{expt}}=\frac{V_{\text{out}}}{R_{\text{FB}}C}, \tag{3}$$

where $(d\Phi/dt)_{\text{expt}}$ is the instantaneous time potential derivative sensed by the probe, in units of V s^{-1} (the probe potential is always kept at zero). C is the capacitive coupling constant and equal to 0.25 pF (see below). The drop velocity was estimated by making the drop fall alongside two probes in tandem. The sensing region of the probes was, in this case, deeply recessed inside a grounded carcass in order to eliminate long distance charge sensing. By doing this we could obtain two reasonably sharp signals permitting to identify the time interval related to the drop passage between the two probes in tandem. Distances from the drop origin to the sensor varied from 30 to 42 cm, depending on the experiment.

The capacitive coupling constant C of the system drop +sensor was estimated by measuring the response to a falling drop of known electric charge (see below). A drop with 0.27 pC (measured previously by integrating the current versus time signal) was made to fall through the sensing probe. A theoretical ($\partial_t\Phi=\partial\Phi/\partial t$) curve was then generated from the known values of the sensor geometry, drop size, charge, and velocity. This curve was compared, at its maximum, with the experimentally determined through Eq. (3) curve from which the value of C was determined as $C=0.25$ pF with $R_{\text{FB}}=5\times10^{10}\ \Omega$.

Water employed in the experiment was obtained in a de-ionization apparatus (NANO pure from Barnstead) and had resistivity of 0.18 M$\Omega\times$m.

III. MEASUREMENT OF TOTAL DROP CHARGE

Measurement of total drop charge was performed without a capacitor in the drop path (only devices 0,1,3), using a procedure similar to the one employed by MacLatchy and Chipman (1990)[2] in measuring the charge of high-speed metallic projectiles.

The drop charge q is then given by

$$q=\int I_{\text{inj}}\,dt. \tag{4}$$

Usually the integration was performed on the first half of the curve, but integration of the second half gave almost identical values.

The voltage output of the amplifier was acquired by an analog-to-digital (A/D) interface (Labmaster type) and fed onto a 386-based computer. The software AXOTAPE version 2 was used for the acquisition.

In order to test the charge measuring system, water drops were produced with the cavity (device 1) maintained at different potentials. The charge in the drops was then determined by integrating the current versus time curves, Eq. (4). Knowing the drop radius a, the potential of the drop Φ is calculated from

$$\Phi=\frac{q}{4\pi\epsilon_0 a}. \tag{5}$$

Typical water drops had a mass of 13.04 mg (as inferred from the weight of 50 drops) from which a radius of 1.46 mm was inferred assuming spherical symmetry and density 1 g/cm^3. The predicted potential was found to correlate well with the potential imposed in the cavity (device 1), as shown in Fig. 2. Initial tests were conducted in which the charge of a same drop was simultaneously determined using two different procedures:

(1) by integrating the current versus time curve (as described above) and
(2) by using a Keithley 616 digital electrometer as a coulombmeter. The correlation between the two measurements was excellent indicating that the sensor ring detects most of the charge of the drop. Different sensor geometries were tested, and the measured charge, using Eq. (4), was found to be independent of the particular sensor geometry within reasonably wide limits.
(3) In order to produce drops of near zero charge (see below), the cavity potential is changed (with the capacitor in the discharged condition), until the falling drops produce a negligible signal on the sensor output.
(4) Multipole charge induction was accomplished by letting drops with zero net charge fall through the capacitor (device 2) typically maintained at 30 V with 67 mm plate separation. The sensor probe is placed between the plates at mid-distance between them. Initially the voltage of the capacitor is fixed to zero and device 1 is adjusted until no signal is detected by the sensor. Then, with voltage at device 1 kept unchanged, capacitor voltage is brought to values ranging from zero to 30 V, in either polarity.

IV. EXPERIMENTAL RESULTS

A. Monopolar drops

When, in initial tests, drops were formed without device 1 attached, we found that they always possessed a net charge in the few pC range. Since many different sources of a dc field could be present inside the cage, affecting the electrification of the nascent drops, we did not pursue this problem any further. By later keeping the forming drops inside device 1 we could, at the same time, shield them from the external sources of charge and impose a known electrical potential to the nascent drop. In this way we could produce drops of positive or negative charge by maintaining the surrounding ring (device 1) at respectively negative or positive voltage. The signals produced by positive and negative drops were essentially mirror images from each other. Typical signal from positively charged drops (capacitor absent or at zero voltage) are shown in Figs. 3(a) and 3(b), for drops produced with the surrounding ring (device 1) at negative voltage. It can be seen that the drop charge or potential has the opposite sign of the ring potential.

With a discharged capacitor in the path the signal is shown in Fig. 3(b) and shows, besides the expected biphasic response, two tail currents. Comparison between this signal and that obtained without the capacitor in the path [Fig. 3(a)] shows that the tail currents are a result of the shielding provided by the capacitor plates, which cuts the signal when the drop is outside the space delimited by the plates. As is shown below, this shielding effect is not relevant for drops having zero net charge, as their electrical influence is short reached.

B. Multipolar drops

By adjusting the voltage in the upper ring (device 1) we could obtain drops that produced essentially zero signal (net charge in the few fC range). We refer to these drops as zero net charge drops (ZNCD). When ZNCD transverse a charged capacitor (10–30 V with the lower plate at the given voltage and upper plate grounded), the previously near zero signal changes to a well-defined four-phase signal having a minimum of 50 times signal/noise ratio for individual tracings. With the lower capacitor plate at positive voltage there is a first positive deflection, followed by a negative deflection, then a high-amplitude positive deflection, and finally a negative deflection. The signal amplitude increases proportionally to increasing capacitor voltage. The pattern symmetrically reverts with voltage reversion at any given voltage from 10 to 30 V [Figs. 4(a) and 4(b)].

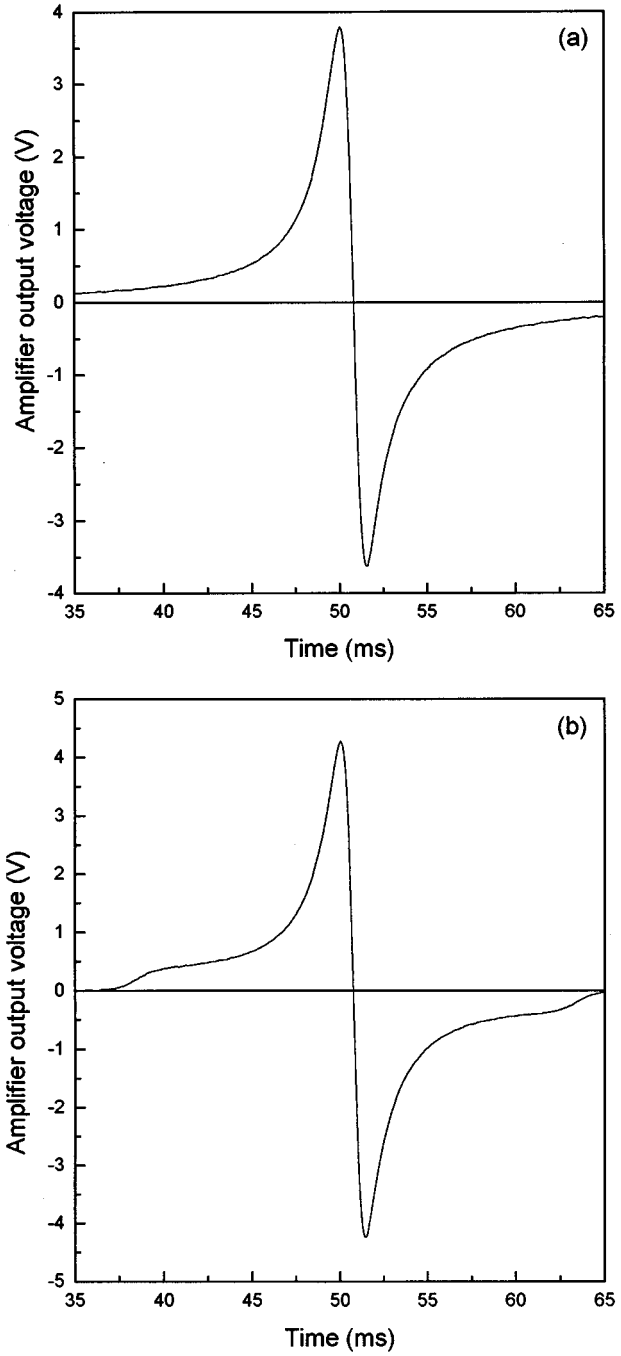

FIG. 3. (a) Signal from a positively charged drop of 0.27 pC (surrounding ring at negative voltage), no capacitor in the path. (b) Signal from a positively charged drop with discharged capacitor in the path.

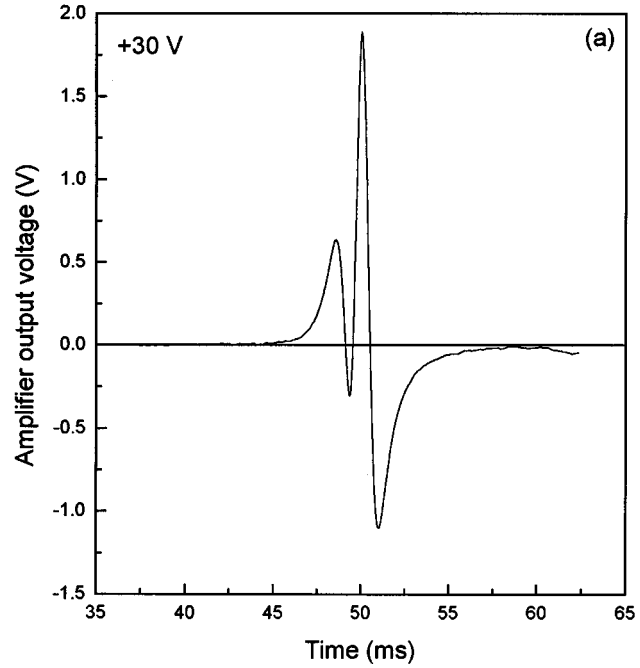

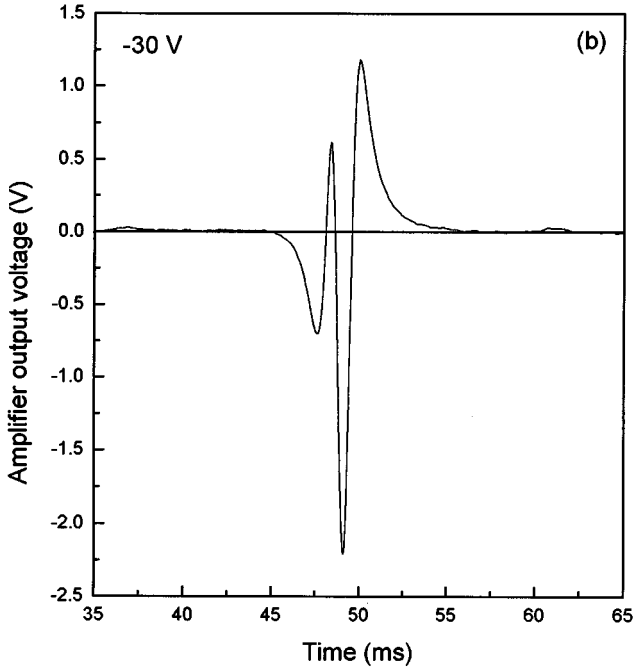

FIG. 4. The figures corresponding to negative voltages are mirror images with those with positive voltages.

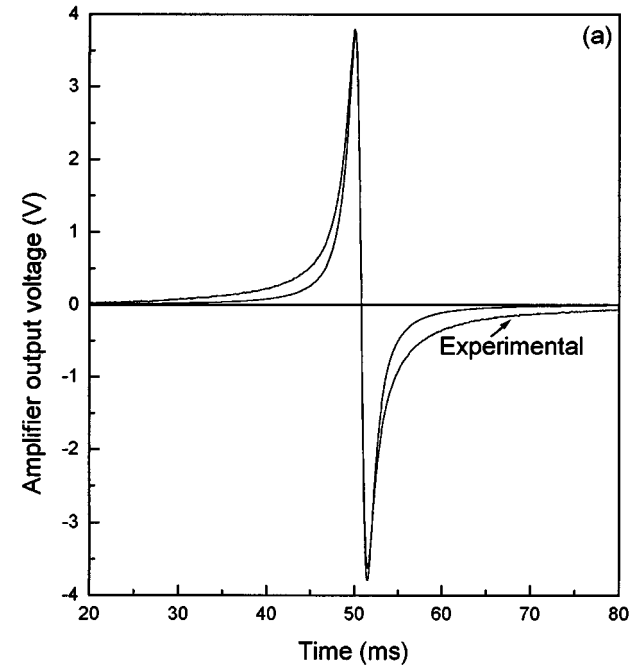

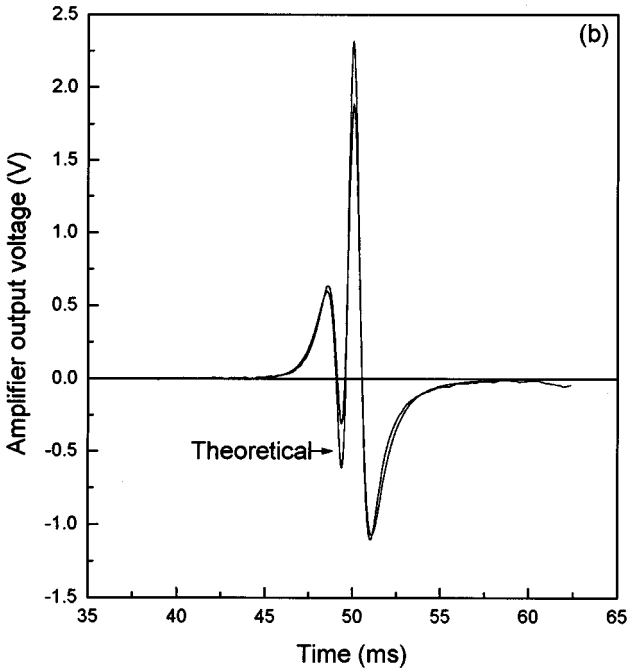

FIG. 5. (a)Monopolar fitting. (b) Multipolar fitting with $V=+30$ V.

C. Curve fitting

1. Fitting for the monopolar distribution

Curve fitting for charged drops falling with no capacitor in the path were undertook using the equation [see Eqs. (14) and (15) in Sec. V]

$$\partial_t \Phi[z(t)] = -\frac{1}{4\pi\epsilon_0} v_z (z^2+l^2)^{-3/2} zq. \tag{6}$$

The experimental curve is the average of 30 successive signals (see Fig. 5). As seen in Fig. 5(a) we could obtain reasonable fittings using a theoretical free falling water drop having a single charge located at the center.

2. Fitting for the multipolar distribution ZNCD

The experimental curve used for the fitting with a theoretically derived signal is the average of at least 30 successive individual signals either for the monopole or for the multipole. A program in QBASIC was employed to compare the experimental curve to different theoretically generated ones. In the derivation of the theoretical signal the following principles were used:

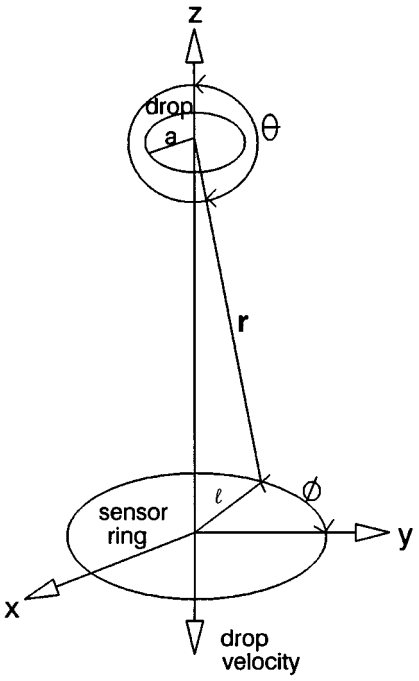

FIG. 6. Drop coordinates.

(1) The theoretical drop falls freely in vacuum but a correction is made to fit its velocity at the sensor position, with the velocity of the experimental drop;
(2) the theoretical drop does not change its net charge during the flight;
(3) the system has azimuthal symmetry;
(4) the theoretical sensor ring has no peduncle whereas the experimental has one.

Considering our experimental condition with the charge on the drop equal zero, $q=0$, Eq. (15) (see Sec. V) transforms,

$$\partial_t\Phi[z(t)]=-\frac{1}{4\pi\epsilon_0}\,v_z\Big((z^2+l^2)^{-3/2}p_z+(z^2+l^2)^{-5/2}\times(-3z^2p_z+Q_{zz}z)-\frac{5}{2}\,(z^2+l^2)^{-7/2}z(Q_{xx}l^2+Q_{zz}z^2)\Big)+\cdots. \tag{7}$$

The comparison with the experimental curve gives a best fitting when the multipolar parameters are the following: $p_z=1.20\times10^{-16}$ C m, $Q_{xx}=4.10\times10^{-19}$ C m^2, $Q_{zz}=27.\times10^{-19}$ C m^2.

V. THEORY

Potential spectrum of a falling charged droplet: The drop coordinates are shown in Fig. 6: When the droplet falls in the z direction, the detector which has a circular shape of radius l surrounding the z axis senses the temporal derivative of the potential $(\partial_t\Phi=\partial\Phi/\partial t)$. The potential outside the droplet can be written as a multipole expansion (see for instance Jackson[3]),

$$\Phi(\mathbf{x})=\frac{1}{4\pi\epsilon_0}\left(\frac{q}{r}+\frac{\mathbf{p}\cdot\mathbf{x}}{r^3}+\frac{1}{2}\sum_{i,j}\,Q_{ij}\,\frac{x_ix_j}{r^5}+\cdots\right). \tag{8}$$

In Eq. (6) q is the total charge, or monopole moment, $\mathbf{p}$ is the electric moment,

$$\mathbf{p}=\int\mathbf{x}'\rho(\mathbf{x}')d^3x', \tag{9}$$

and Q_{ij} is the quadrupole moment tensor,

$$Q_{ij}=\int(3x_i'x_j'-r'^2\delta_{ij})\rho(\mathbf{x}')d^3x'. \tag{10}$$

Expanding Eq. (6) up to the quadrupolar term we obtain

$$\Phi(\mathbf{x})=\frac{1}{4\pi\epsilon_0}\left(\frac{q}{r}+\frac{1}{r^3}\,(p_xx+p_yy+p_zz)+\frac{1}{2r^5}\,(Q_{xx}x^2+Q_{yy}y^2+Q_{zz}z^2+2Q_{xy}xy+2Q_{xz}xz+2Q_{yz}yz)+\cdots\right). \tag{11}$$

Adapting the former equation to our experimental setup (Fig. 5), $r=(z^2+l^2)^{1/2}$, we have

$$\mathbf{\Phi}[z(t)]=\frac{1}{4\pi\epsilon_0}\left((z^2+l^2)^{-1/2}q+(z^2+l^2)^{-3/2}(p_xx+p_yy+p_zz)+\frac{1}{2}\,(z^2+l^2)^{-5/2}(Q_{xx}x^2+Q_{yy}y^2+Q_{zz}z^2+2Q_{xy}xy+2Q_{xz}xz+2Q_{yz}yz)+\cdots\right). \tag{12}$$

The temporal derivative of the potential will be

$$\partial_t\mathbf{\Phi}[z(t)]=\frac{1}{4\pi\epsilon_0}\,v_z\Big((z^2+l^2)^{-3/2}(-zq+p_z)+(z^2+l^2)^{-5/2}[-3z(p_xx+p_yy+p_zz)+Q_{zz}z+Q_{xz}x+Q_{yz}y]-\frac{5}{2}\,(z^2+l^2)^{-7/2}z(Q_{xx}x^2+Q_{yy}y^2+Q_{zz}z^2+2Q_{xy}xy+2Q_{xz}xz+2Q_{yz}yz)\Big)+\cdots. \tag{13}$$

Applying the condition of azimuthal symmetry, $p_x=p_y=0$ and $Q_{i,j}=0$ for $i\neq j$ with $Q_{xx}=Q_{yy}$, Eqs. (13) transform,

$$\partial_t\mathbf{\Phi}[z(t)]=\frac{1}{4\pi\epsilon_0}\,v_z\Big((z^2+l^2)^{-3/2}(-zq+p_z)+(z^2+l^2)^{-5/2}(-3z^2p_z+Q_{zz}z)-\frac{5}{2}\,(z^2+l^2)^{-7/2}z[Q_{xx}(x^2+y^2)+Q_{zz}z^2]\Big)+\cdots. \tag{14}$$

Considering the detector positioned at $x=l$, $y=0$, then Eq. (14) transforms,

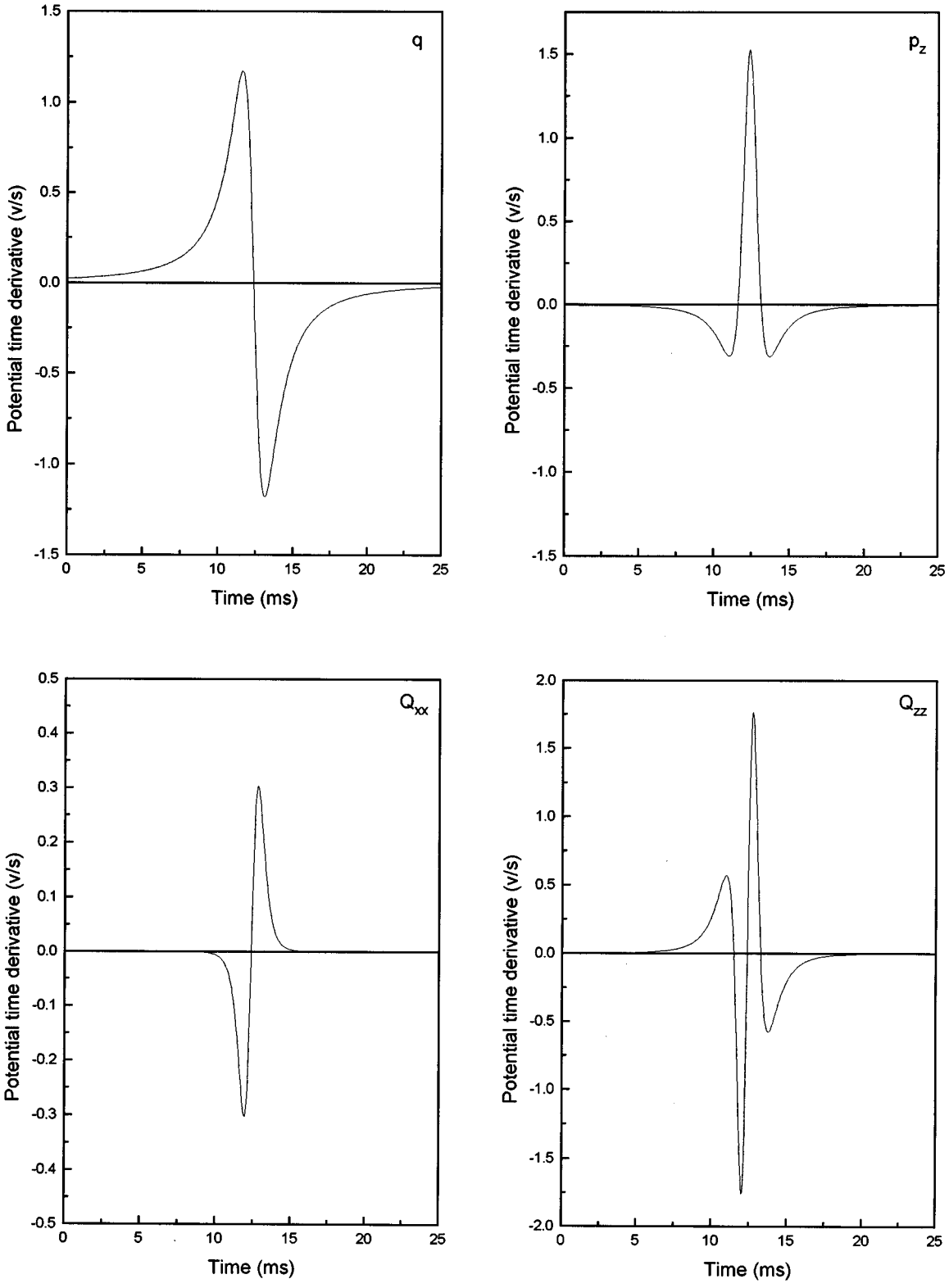

FIG. 7. Theoretical multipolar contributions to the temporal derivative of the potential.

$$\partial_t \mathbf{\Phi}[z(t)] = \frac{1}{4\pi\epsilon_0} v_z \Big((z^2+l^2)^{-3/2}(-zq+p_z) + (z^2+l^2)^{-5/2}(-3z^2 p_z + Q_{zz} z) - \frac{5}{2}(z^2+l^2)^{-7/2} z (Q_{xx} l^2 + Q_{zz} z^2) \Big) + \cdots . \tag{15}$$

In the former equations the coordinate z and the velocity v_z have to be replaced by

$$z = H - v_{0z}t - \tfrac{1}{2}gt^2 \quad \text{and} \quad z_t = -(v_{0z} + gt). \tag{16}$$

in order to visualize the experimental spectral patterns.

In Fig. 7 are shown the different multipolar contributions to the temporal derivative of the potential.

VI. DISCUSSION

Despite many previous works[1,2] that report experimental procedures for measuring electrical charges in free moving objects, there are no consistent data describing the spatial charge distribution within or on the surface of water drops immersed in air. Tomíc and Kallay studied the charge distribution inside droplets immersed in oil, and described a distribution based on a Poisson–Boltzmann equation.[4]

Falling drops are adequate systems to study spatial charge distribution since they provide, at the same time, an object that is electrically insulated and moving relative to a stationary sensing device. The present work provides experimental evidence that the electrical charge in a water drop falling in the direction of an applied electric field is distributed in a multipolar pattern. Our results were made possible only because a means of nullifying the total charge of the drops was employed, otherwise the net drop charge would have masked the much smaller signal from the multipolar charge distribution. Although the capacitor (device 2) has two holes for entry and exit of the drops the field can be, on a first approximation, considered uniform along the drop path.

The theoretical fittings for our experimental results are not in accordance, however, with what one would expect for a dielectric sphere in a uniform electric field, in which case a pure dipolar pattern would be observed. The present results can be interpreted along two main lines of reasoning. The first sees the macroscopic charge distribution on the drop and the second relates the experimental signal to molecular parameters of the water molecule.

The results derived in Sec. V, namely Eq. (7), apply both to a phenomenological macroscopic charge distribution in an isotropic, homogeneous body and to a set of molecular electrical multipoles.

In a uniform electric field, the water drop can be taken as a sphere having a dipole moment of[3]

$$p = 4\pi\epsilon_0 \left(\frac{\epsilon - 1}{\epsilon + 2} \right) a^3 E. \tag{17}$$

If we consider the possibility that even purified water to a resistivity of 0.18 $\mathrm{M}\Omega$ m has a dielectric relaxation time in the range of μs,[5] we have that, in the time scale of the imposed perturbation, the water drop would behave like a conductor which permits writing $\epsilon \to \infty$ making the premultiplier in Eq. (17) approach 1. With $E = 447$ V m^{-1} and $a = 0.146$ cm, $p = 1.54 \times 10^{-16}$ C m which is the order of the experimental fitting value (1.20×10^{-16} C m). Another possibility for purer water with $\epsilon = 80$ would give $p = 1.49 \times 10^{-16}$ C m.

The contribution of the quadrupolar moment Q_{zz} of the water molecule is estimated from the reported values of quadrupolar moments and the number of water molecules contained in the drop. Due to the random orientation of the molecules around the z axis the only component of the quadrupole moment expected to result is Q_{zz}. With respect to the existence in the fitting of Q_{xx} we believe that this is due to the conducting peduncle that links the annulus part of the sensing device to the probe (see Fig. 1), which breaks the random orientation of the molecules in the radial plane.

From the reported value of $Q_{zz} = 8.34 \times 10^{-40}$ C m^2 (see Ref. 6) the combined quadrupolar moment of the individual water molecules in the drop is given by

$$8.34 \times 10^{-40} \times 4.35 \times 10^{20} = 3.63 \times 10^{-19} \text{ C m}^2,$$

which is to be compared with the experimental fitting parameter $Q_{zz} = 27 \times 10^{-19}$ C cm^2.

In conclusion, the experimental curves can be fitted to the theoretical ones generated by an electric multipolar object, falling through the sensor ring. There is evidence that the measured charge distribution in this object is due to the contribution of the field-oriented water molecule multipoles.

ACKNOWLEDGMENTS

This work was partially supported by the Conselho Nacional de Desenvolvimento Científico e Tecnológico (CNPq Brazil) and Fundação de Amparo à Pesquisa do Estado de São Paulo (FAPESP).

[1] Lord Kelvin, Atmospheric Electricity, Royal Institute Lecture Papers on Electrostatics and Magnetism, 1860, pp. 208–226.
[2] C. S. MacLatchy and H. A. Chipman, Am. J. Phys. **58**, 811 (1990).
[3] J. D. Jackson, *Classical Electrodynamics* (Wiley, New York, 1962).
[4] M. Tomíc and N. Kallay, J. Phys. Chem. **96**, 3874 (1992).
[5] J. B. Hasted, *Aqueous Dielectrics* (Chapman and Hall, London, 1973), p. 167.
[6] J. Verhoeven and A. Dynamus, J. Chem. Phys. **52**, 3222 (1970).